Neuromuscular Disorders 58 (2026) 106296

Contents lists available at ScienceDirect

Neuromuscular Disorders

journal homepage: www.elsevier.com/locate/nmd

Identification of novel potentially causative *RYR1* variants in individuals with malignant hyperthermia susceptibility

Daniela Rossi [a,b,*], Carlotta Pranzo [a], Sara Roccabianca [a], Lucia Galli [b], Alfredo Orrico [b], Giovanna Sorbello [b], Vincenzo Tegazzin [b], Pasquale D'Onofrio [c], Armando Fucci [c], Salvatore Quarta [c], Stefano Perni [a], Egidio Maria Rubino [a], Matteo Serano [a], Gianna Berti [d,e], Diego Lopergolo [e], Alessandro Malandrini [d,e], Filip Van Petegem [f], Vincenzo Sorrentino [a,b]

[a] Department of Molecular and Developmental Medicine – University of Siena, Siena, Italy
[b] Program of Molecular Diagnosis of Rare Genetic Diseases, Azienda Ospedaliera Universitaria Senese, Siena, Italy
[c] Perioperative Anesthesia and Reanimation Unit, Azienda Ospedaliera Universitaria Senese, Siena, Italy
[d] Department of Medicine, Surgery and Neuroscience – University of Siena, Italy
[e] Neurology and neurometabolic disease - Azienda Ospedaliera Universitaria Senese, Siena, Italy
[f] Department of Biochemistry and Molecular Biology, the Life Sciences Centre, University of British Columbia, Vancouver Canada

ARTICLE INFO

Keywords:
Malignant hyperthermia
Calcium homeostasis
Skeletal muscle
Calcium channel

ABSTRACT

Malignant Hyperthermia Susceptibility (MHS) is a pharmacogenetic disorder triggered by volatile anesthetics and muscle relaxants, leading to a hypermetabolic reaction in skeletal muscle that can be fatal if untreated. Diagnosis relies on an *in vitro* contracture test (IVCT) on muscle biopsy and/or genetic testing for pathogenic variants in the *RYR1* gene, which accounts for most cases; less frequently, variants are found in *CACNA1S* and *STAC3*. However, unlike the IVCT, genetic testing is limited by the large number of *RYR1* variants classified as of uncertain significance (VUS), preventing it from fully replacing the IVCT.

We report data from 250 MHS individuals followed over 20 years, in whom 100 *RYR1* and 3 *CACNA1S* variants were identified. Among the *RYR1* variants, 81 were previously reported and 19 were novel, all classified as VUS according to European Malignant Hyperthermia Group (EMHG) and Variant Curation Expert Panel (VCEP) criteria. Similarly, of the 3 *CACNA1S* variants, 1 was previously reported and 2 were classified as VUS.

The reporting of novel variants is crucial for improving the accuracy and consistency of variant classification, thereby supporting a more precise interpretation of their clinical significance.

1. Introduction

Malignant hyperthermia susceptibility (MHS) is a rare pharmacogenetic disorder that can cause a severe hypermetabolic state following exposure to succinylcholine and volatile anesthetics. This reaction, which can be fatal if not treated promptly with the muscle relaxant dantrolene, is caused by a massive release of Ca^{2+} in skeletal muscles, resulting in increased carbon dioxide production, hyperthermia, muscle rigidity, rhabdomyolysis and acidosis [1–5].

MHS is primarily caused by rare variants in the ryanodine receptor type 1 (*RYR1*) gene; less frequently (in about 1 % of MHS individuals) causative variants can be found in the *CACNA1S* and in the SH3 And Cysteine Rich Domain 3 (*STAC3)* genes [6–9]. Analysis of the general population suggests that the prevalence of individuals carrying pathogenic MHS variants is around 1:1,000 [6,7,10], while the incidence of clinical MHS episodes is estimated around 1:10,000 for pediatric and 1:100,000 for adult anesthesia. The observed discrepancy is mainly explained by a low penetrance of the clinical phenotype and/or the presence of additional factors that may either favor or prevent the occurrence of a MHS episode [4].

Recent research suggests that MHS can be part of a broader spectrum of *RYR1*-related disorders, which are all characterized by dysfunctional Ca^{2+} release from the endoplasmic/sarcoplasmic reticulum and a general disruption of Ca^{2+} homeostasis, which variably impacts skeletal muscle cell function [11–14]. These disorders can also manifest as MHS-like episodes without anesthesia, including muscle cramping and exertional rhabdomyolysis [15–20].

MHS can be diagnosed through an in vitro contracture test (IVCT), on

* Corresponding author at: University of Siena, Department of Molecular and Developmental Medicine, Via Aldo Moro, 2, 53100 Siena, Italy.
E-mail address: daniela.rossi@unisi.it (D. Rossi).

https://doi.org/10.1016/j.nmd.2025.106296
Received 24 June 2025; Received in revised form 7 November 2025; Accepted 24 November 2025
Available online 25 November 2025

a muscle biopsy or through genetic testing. The decision to pursue IVCT or genetic screening is made on a case-by-case basis following clinical evaluation and genetic counseling according to the European Malignant Hyperthermia Group (EMHG) guidelines (https://www.emhg.org) [3,4]. Although more invasive for patients and more demanding for diagnostic laboratories, the IVCT currently remains the gold standard for diagnosing MHS with high sensitivity and specificity [3,4,21]. Genetic testing, performed primarily through Next Generation Sequencing (NGS), is complicated by the huge number of *RYR1* variants of unknown significance (VUS) present in this large gene. This makes it difficult to definitively classify variants as pathogenic or benign and explains why genetic testing has not yet fully replaced the IVCT. To address this challenge the EMHG and ClinGen Variant Curation Expert Panel (VCEP) (ClinGen, https://www.ncbi.nlm.nih.gov/clinvar/submitters/508072/) have developed scoring matrices and guidelines to classify variants based on recommendation from the American College of Medical Genetics and Genomics and Association for Molecular Pathology (ACMG/AMP), which has been adapted to MHS [6,7,9]. The EMHG has identified 68 pathogenic or likely pathogenic variants (66 in *RYR1* and 2 in *CACNA1S*), while ClinGen has classified 86 *RYR1* variants as pathogenic or likely pathogenic, 219 were referred as VUS and 30 as likely benign or benign [6,7].

Given that classification of a variant as pathogenic or likely pathogenic requires the fulfillment of multiple criteria, a considerable number of variants remain classified as VUS. Access to data from different laboratories can substantially aid in determining the diagnostic significance of specific variants, either by confirming their current classification as VUS or by supporting their reclassification as benign/likely benign or likely pathogenic/pathogenic.

Accordingly, with the aim of expanding the catalog of *RYR1* and *CACNA1S* variants associated with MHS, we conducted a critical analysis, according to EMHG and VCEP criteria, of the genetic findings and clinically relevant information available for probands and their families from a large cohort of individuals referred to our diagnostic center at the Azienda Ospedaliera Universitaria Senese (AOUS) over the past 20 years. Individuals were evaluated by IVCT and/or genetic testing using a panel that included *RYR1, CACNA1S, STAC3*, and 16 additional genes encoding proteins involved in the regulation of Ca^{2+} homeostasis, mutations in which may potentially trigger an MHS crisis [22,23].

As a result of this comprehensive analysis, in addition to confirming 81 previously reported variants, we identified 19 novel variants in *RYR1* and 2 in *CACNA1S*, which, according to current guidelines and available evidence, are classified as VUS. Future studies will be required to confirm or refine the classification of these novel variants.

2. Methods

We conducted a retrospective study of MHS and MHS-suspected individuals who were evaluated at the Azienda Ospedaliera Universitaria Senese and who underwent IVCT, genetic analysis and/or histological analysis of muscle biopsy between 2004 and 2024. When available, relatives carrying familial *RYR1* variants (with a positive IVCT) were also included. Informed consents were obtained at the time of the IVCT and/or genetic analysis. IVCT was performed on muscle biopsies from vastus lateralis mounted in contracture chambers and exposed to increasing concentrations of halothane and caffeine according to the protocol of the EMHG [3].

2.1. Molecular genetic studies

Genomic DNA was extracted from peripheral blood leucocytes following standard methods [22]. *RYR1* genomic structure and intron boundary sequences were deduced from the Homo sapiens chromosome 19 genomic contig NT_011109 and cDNA sequence NM_000540.1. From 2004 to 2016 the coding regions (exons 1–106) of the *RYR1* gene, including splice sites, were screened by Denaturing High Performance Liquid Chromatography (DHPLC) screening and, later, by DNA sequencing of all 106 exons of the *RYR1* gene [23]. Starting from 2016, NGS and standard Sanger sequencing (Applied Biosystems 3500 Series Genetic Analyzer) were applied using a panel with 19 genes (*RYR1, CACNA1S, MYH7, SEPN1, ATP2A1, STIM1, STAC3, ASPH, TRDN, KCNA1, TRPC3, HRC, JPH2, SRL, ORAI1, SPEG, FXYD1, PLB, JPH1, SLN)* (Ion GeneStudio™ S5 System, Thermo Fisher Scientific). All available DNAs from 2004 to 2016 have been re-sequenced by NGS to identify variants that may have been missed by previous analysis. All identified *RYR1* variants were first assessed to determine if they were diagnostic (i.e., pathogenic or likely pathogenic) according to EMHG/VCEP criteria. Variants not included in the submissions to EMHG/VCEP were analyzed by public databases, prediction algorithm software and web-based platforms including PolyPhen-2 (http://genetics.bwh.harvard.edu/pph2/index.shtml) [24], Rare Exome Variant Ensemble Learner (REVEL) [25], Alamut Visual Plus (v1.8.1, SOPHiA Genetics, USA) [26], Franklin by Genoox (https://franklin.genoox.com - Franklin by Genoox), ClinVar (https://www.ncbi.nlm.nih.gov/clinvar/), genome aggregation database (gnomAD, https://gnomad.broadinstitute.org), LOVD v.3.0 - Leiden Open Variation Database (https://www.lovd.nl) and VarSome (http://varsome.com/) [27]. REVEL scores were considered as follows: above 0.932 = strong pathogenic evidence; between 0.773 and 0.932 = moderately pathogenic; between 0.644 and 0.773 = supporting pathogenic; from 0.183 to 0.29 = supporting benign; between 0.016 and 0.183= moderately benign; from 0.003 to 0.016 strongly benign and score below 0.003 very strongly benign. According to PolyPhen-2, score ranges from 0.0 (tolerated) to 1.0 (deleterious). Variants with scores of 0.0 to 0.15 are predicted to be benign; values from 0.15 to 1.0 are classified as possibly damaging; values from 0.85 to 1.0 are more confidently predicted to be damaging [26].

2.2. Histological and histochemical studies

Muscle specimens from *Vastus lateralis* were processed using standard methodologies. Frozen sections were stained with hematoxylin-eosin, Gomori's modified trichrome reaction, periodic acid-Schiff (PAS), oil red, nicotinamide adenosine dinucleotide reductase (NADH-TR), nicotinamide adenosine dinucleotide diaphorase (DPNH), succinate dehydrogenase (SDH), ATPase staining at pH 10.4, 4.7 and 4.3, cytochrome c oxidase (COX) and acid phosphatase, as previously described [28].

2.3. Structural analysis

To analyze and visualize the potential impact of the variants, a high-resolution (2.45Å) cryo-EM structure of rabbit RyR1 was used (PDB ID: 7TZC) [29]. Pymol (Schrodinger) was used to visualize the overall location and to mutate the residues. When no clashes were present, a rotamer with the least number of clashes was selected. These rotamers are only for visual representation, as gauging the precise details, as well as any impact of the variants on the local and global conformations requires experimental structures to be obtained (e.g. as shown before) [30,31].

3. Results

3.1. Study cohort information

Data from 612 individuals who underwent both IVCT and genetic analysis, and from 699 individuals who underwent only genetic analysis were collected from 2004 to 2024 (Figs. 1 and 2). We analyzed 158 families, ranging from 2 to 84 members each, for a total of 866 individuals (Fig. 1C); the remaining 445 were sporadic cases. Of the 612 individuals tested by IVCT, a total of 250 (158 males and 92 females, aged 42.8±15.4) resulted as MHS while the remaining 362 individuals (200 males and 162 females, aged 43.5±15.9) were classified as

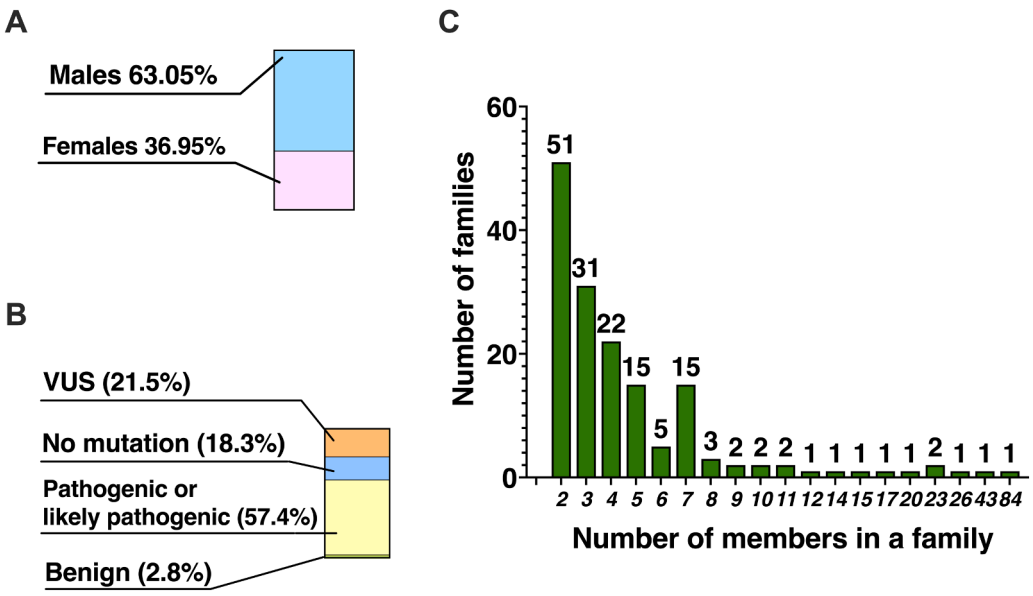

Fig. 1. Study Cohort Information. A. Sex distribution of MHS individuals. **B.** Classification of *RYR1* variants identified in MHS individuals: pathogenic and likely pathogenic variants were classified according to EMHG/VCEP matrix scores; VUS indicates variants of uncertain significance according to EMHG/VCEP matrix scores; "no mutation" includes patients whose genetic analysis revealed no variants in RYR1, CACNA1S or STAC3; Benign variants were classified according to EMHG/ClinGen matrix scores. **C.** Family size distribution.

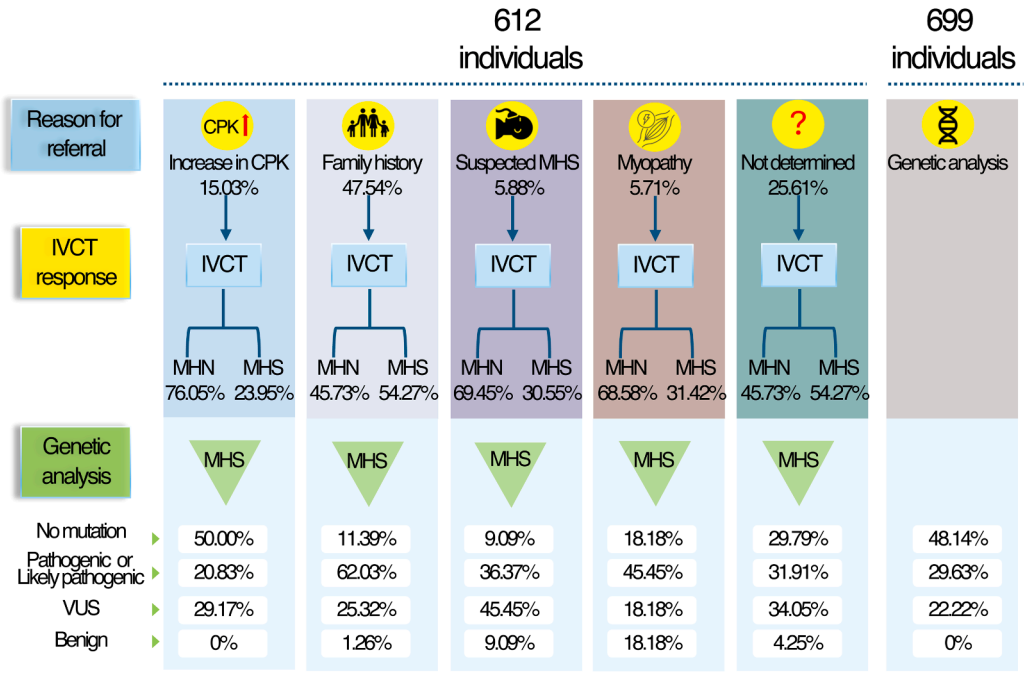

Fig. 2. Diagnostic Workflow for Malignant Hyperthermia Susceptibility (MHS). 612 individuals underwent both IVCT and genetic analysis, while 699 individuals underwent only genetic analysis for MHS diagnosis. The 612 individuals were grouped according to the reason for referral to our center: a) elevated CPK: this group includes individuals with idiopathic increase in resting CPK levels higher than 200 U/l; b) family history of MHS: this group includes individuals with relatives who encountered an adverse event during general anesthesia, or relatives who resulted positive at the IVCT (but did not carry a pathogenic or likely pathogenic variant at the time of diagnosis), or relatives who were diagnosed or suspected for a *RYR1*-related myopathy; c) Suspected MH event: this group includes individuals with a personal adverse event during general anesthesia; d) Suspected myopathy: this group includes individuals who report neurological signs of myopathy or muscle-related symptoms; e) not determined includes individuals for whom anamnestic data are not available. Muscle biopsies underwent histological analysis. Individuals who resulted MHN at the IVCT were no further analyzed. Individuals who resulted MHS at the IVCT were analyzed by NGS using a panel of 19 genes. Classification of *RYR1* variants identified in MHS individuals: pathogenic and likely pathogenic variants were classified according to EMHG/VCEP matrix scores; VUS indicates variants of uncertain significance according to EMHG/VCEP matrix scores; "no mutation" includes patients whose genetic analysis revealed no variants in *RYR1, CACNA1S* or *STAC3*. The 699 individuals who referred to our center only for genetic analysis include individuals with relatives carrying a pathogenic or likely pathogenic variant in *RYR1* or *CACNA1s* who do not require IVCT, individuals with a suspected myopathy or individuals for whom anamnestic data are not available.

Malignant Hyperthermia Negative (MHN) (Fig. 1A). Among the 250 MHS individuals, 187 were positive to both caffeine and halothane, 45 were positive only to halothane and 18 were positive only to caffeine. 159 of the MHS individuals had a family history of MHS, 11 were referred to our diagnostic center following an adverse event during general anesthesia, while the other probands reported non-specific signs such as an increase in resting Creatine Phospho Kinase (CPK) levels (23 individuals), a suspected myopathy or other muscle-related symptoms (11 individuals); for the remaining 47 individuals, anamnestic data were not available. (Fig. 2). Clinical symptoms, when present, were heterogeneous and ranged from muscle cramps and myalgia to rhabdomyolysis. No correlation was observed between CPK levels and positivity to the IVCT, since most individuals reporting an increase in CPK levels resulted as MHN at the IVCT (76.05 % MHN vs 23.95 % MHS individuals) (Fig. S1). Association of MHS with increase in CPK levels is still controversial: some authors reported a positive association [32–34], while others showed no close correlation between increase in CPK levels and MHS susceptibility [35,36]. According to the guidelines of the EMHG, utility of creatine kinase levels is limited because of a lack of sensitivity and specificity. Nevertheless, they recommend investigation of MHS susceptibility in all patients with persistent hyperCKaemia, where full neurological evaluation has excluded other causes.

3.2. Histological alteration in skeletal muscles

Biopsies from 403 individuals, including 93 MHS and 330 MHN

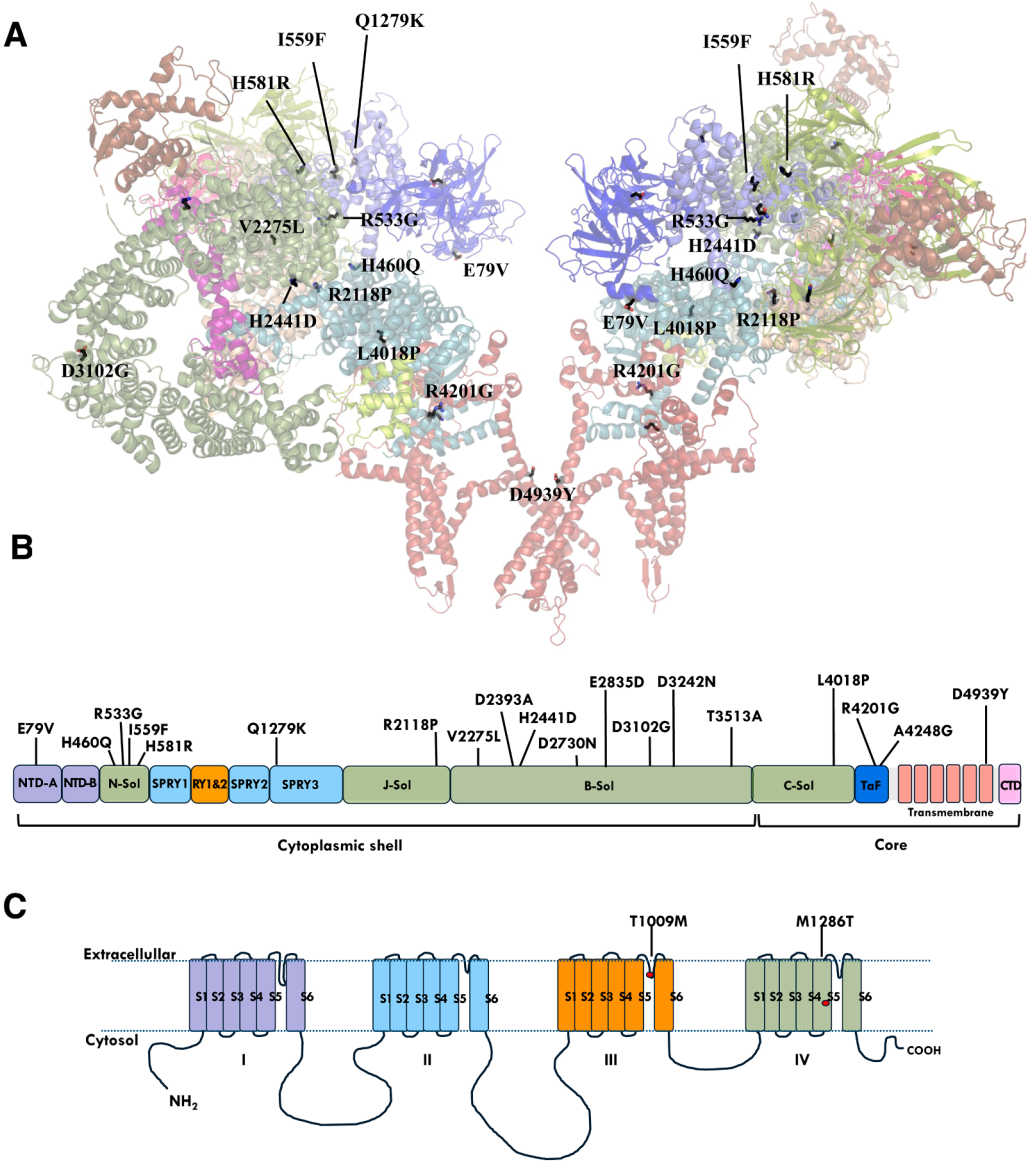

Fig. 3. Mapping of *RYR1* and *CACNA1S* sequence variants on channels structure. A. Ribbon diagram of the rabbit RYR1 cryo-EM structure (PDB ID: 7TZC) with variants shown as black sticks and numbered according to the human RyR1 variant position. For clarity, only two RyR1 protomers are shown. Different colors identify different regions of RyR1, specifically: dark blue: N-terminal domains (NTD-A and NTD-B); light blue: N-terminal solenoid (N-Sol); light green: SPRY domains; brown: Repeat12 and Repeat34 domains; cyan: central solenoid (C-Sol); beige: junctional solenoid (J-Sol); red: transmembrane region, S2-S3 linker and C-terminal domain (CTD); purple: Calmodulin; pink: FKBP12.6. **B.** Localization of *RYR1* sequence variants within RYR1 domains. Domains are represented by square blocks in different colors: dark blue: N-terminal domains (NTD-A and NTD-B); light blue: N-terminal solenoid (N-Sol); light green: SPRY domains; brown: Repeat1&2; junctional solenoid (J-Sol); violet: Bridging solenoid (B-Sol); cyan: central solenoid (C-Sol); dark yellow: Thumb and Forefinger domain (TaF); beige: Red: transmembrane regions and C-terminal domain (CTD). **C.** Localization of *CACNA1S* sequence variants within the structure of the alpha 1S subunit of DHPR. Transmembrane domains are represented by square blocks in different colors. Roman numbers indicate the four homologous repeats that form the alpha 1S subunit. S1-6 indicate helices within each transmembrane domain. Red dots indicate variant position in the alpha 1S subunit structure.

individuals were analyzed for histological alterations. Both MHS and MHN showed a variable range of histological profiles, ranging from a normal muscle biopsy (15.84 % in MHS and 19.70 % in MHN) to myopathic alterations (Table S1). These alterations were observed in more than 85 % of individuals with MHS, regardless of the presence of causative or novel variants in *RYR1*. Similar alterations were also identified in MHN individuals. A significant fraction of MHS and MHN individuals showed a percentage of internal nuclei higher than 3 % (19 MHS individuals and 47 MHN individuals, corresponding to 18.81 % of MHS and 22.97 % of MHN individuals, respectively) suggesting an association with a mild to severe myopathy. Other frequent histological traits included DPNH-positive fibers (3.96 % vs 4.30 % in MHS and MHN individuals, respectively), prevalence of type I fibers (2.97 % vs 0.91 % in MHS and MHN individuals, respectively), glycogen accumulation (1.98 % vs 1.82 % in MHS and MHN individuals, respectively) and moth-eaten fibers (2.97 % vs 1.82 % in MHS and MHN individuals, respectively); finally, absence of NADH-TR positive fibers in MHS individuals were also observed (Table S1). These features partially match with those reported in the literature, which show a variable spectrum of histological alterations including an increase in internal nuclei, unevenness of oxidative staining and increased fiber size variation [13,37].

Our findings support the idea that MHS is primarily a channelopathy with no distinctive structural alterations; when such alterations are present, they are not dissimilar from those observed in MHN individuals.

3.3. Genetic analysis of MHS individuals

Genetic analysis was routinely performed on MHS individuals who tested positive at the IVCT and on patients who referred to our center for a genetic diagnosis of MHS, in the absence of an IVCT response. This analysis led to the identification of 100 different variants in *RYR1* and 3 variants in *CACNA1S,* while no variants were found in the *STAC3* gene (Figs. 1B, 3, Tables 1, 2, Table S2). All variants had an autosomal dominant inheritance pattern. Of the 100 *RYR1* variants identified, 34 were classified as pathogenic and likely pathogenic, 27 as VUS, 10 as benign, 10 of the discovered variants were not included in the EMHG/VCEP guidelines, but reported in the literature, while 19 were novel (Table 1) [7]. 57.4 % of MHS individuals carried a pathogenic or likely pathogenic variant, 21.5 % carried a VUS, 2.8 % carried a benign mutation and 18.3 % individuals had no mutation in *RYR1* or in any of the genes present in the NGS panel was present (Fig. 1B).

Analysis of the *CACNA1S* gene in MHS individuals resulted in the identification of the c.3257 G>A, p.(Arg1086His) variant, which is classified as pathogenic by the EMHG/VCEP guidelines [3] and of two novel mutations, p.(Met1286Thr) and p.(Thr1009Met) (Fig. 3).

3.3.1. Novel variants in RYR1 and CACNA1S

Among the 100 variants identified in the *RYR1* gene, 19 have not been previously reported and are described in the following paragraphs (Fig. 3; Tables 1; 2; Table S3; Fig. S2). In silico analysis by REVEL, PolyPhen-2 and classification according to the EMHG/ACMG/AMP score matrix predicted that all these 19 variants can be considered, based on available information, as VUS.

3.3.1.1. Novel RYR1 variants identified in MHS families. 7 out of the 19 novel variants were identified in 6 families, where at least one individual was confirmed MHS by IVCT.

Variant c.1597C>G in exon 15, resulting in the substitution of an Arg into Gly at residue 533, p.(Arg533Gly), was identified in two siblings, both tested positive for MHS. One of the siblings was tested at the age of 62 and, at the histological level, muscle biopsy presented with internal nuclei, fibers negative for DPNH staining and prevalence of type II fibers. Her brother was tested at the age of 49 and reported an increase in CPK levels (596 U/l) at rest and occasional muscular cramps. At the histological level, muscle biopsy presented with fibers negative for DPNH staining and a prevalence of type II fibers. The c.1597C>G variant is not present in population databases.

A variant, c.6353G>C in exon 39, resulting in the substitution of an Arg into Pro at residue 2118 (p.(Arg2118Pro)) was present in a MHS individual who reports an increase in CPK levels at rest and hypothrophyc fibers at the histological analysis. The same variant was identified in combination with a second novel variant in *RYR1*, c.7321C>G in exon 45, resulting in the substitution of an His into Asp at residue 2441 (p.(His2441Asp)). The two variants were present in three members of a family, where two resulted MHS at the IVCT and the third was MHN, indicating a possible discordance. The proband experienced a MH event during general anesthesia with increase in body temperature and End-Tidal CO_2, acidosis and tachycardia. Muscle biopsies revealed the presence of mitochondrial alteration and prevalence of type II fibers in both MHS and MHN individuals of the family. Both p.(Arg2118Pro) and p.(His2441Asp) are classified as pathogenic by REVEL and damaging by Polyphen-2.

The c.6823G>C substitution in exon 42, resulting in p.(Val2275Leu) amino acid change, was identified in five members of a family where three carriers resulted MHS at the IVCT and the other two did not underwent IVCT test. Muscle biopsies of the three carriers revealed the presence of a heterogeneous histological picture with core-like structures, prevalence of type II fibers or atrophic fibers.

In two members of a family, both positive at the IVCT, variant c.7178A>C in exon 44, resulting in the substitution of an Asp into an Ala at residue 2393, p.(Asp.2393Ala) was identified. The proband reported an increase in body temperature following general anesthesia, an increase in CPK levels at rest and, at the histological level, prevalence of type II fibers. His daughter, who underwent the IVCT at the age of 42, reported myalgia. Histological analysis revealed the presence of some moth-eaten fibers.

The c.8188G>A variant in exon 51 which results in the substitution of an Asp into Asn at residue 2730, (p.Asp2730Asn) was identified in five members of a family, all of whom were classified as MHS based on IVCT results. Two additional family members, who tested negative for the c.8188G>A substitution, resulted as MHN by IVCT. Muscle biopsy of the proband revealed the presence of fiber hypotrophy and prevalence of type II fibers. One of the proband's sons reported the presence of fibers with minicore-like structures and his daughter, who underwent the IVCT at the age of 21, reported the presence of inflammatory cells and moth-eaten fibers; on the contrary, no alteration was present in the muscle biopsy of the proband's daughter, who also carried the p.(Asp2730Asn).

Variant, c.12743C>G in exon 91, p.(Ala4248Gly) was identified in five members of a family, four of which resulted MHS at the IVCT, while the other did not perform the test. The proband experienced a suspected MH reaction during general anesthesia, with acidosis, hypertension, and an increase in body temperature. Histological examination of muscle tissue revealed no abnormalities. In contrast, the proband's two brothers, also carrying the variant, underwent general anesthesia without any reported adverse events. However, the specific anesthetic agent used in these two cases were not documented. They report rare muscular cramps and increased CPK levels at rest. Histological analysis of muscle biopsies from the two proband's brothers (age 48 and 51 years old) revealed the presence of some hyper- and hypotrophic fibers and a prevalence of type II fibers. Muscle biopsy of a MHS younger family member (age 18 years old, proband's nephew) did not reveal evident alterations, although he reported a CPK value of 300 U/l at rest. Despite association with clinical evidence, and IVCT response, REVEL and Polyphen-2 prediction scores do not indicate an evident pathogenic role for this variant.

3.3.1.2. Novel RYR1 variants identified in single MHS individuals. 7 novel variants in *RYR1* were identified in single individuals.

A variant, c.236A>T in exon 3, resulting in the substitution of a Glu into a Val at residue 79, p.(Glu79Val), was identified in one MHS

Table 1
List of novel variants identified in individuals referred to the AOUS from 2004 to 2024. The list includes novel variants classified according to the EMHG/VCEP score matrices. NT=not tested at the in vitro contracture test (IVCT). Domain abbreviations: NTD-A/B, N-terminal domain A/B; N-Sol, N-terminal solenoid; SPRY1/2/3, SP1a/ryanodine receptor domain 1/2/3; J-Sol, junctional solenoid; B-Sol, bridging solenoid; C-Sol, core solenoid; TaF, thumb and forefingers domain; pVSD, pseudo voltage sensor domain; Pore, channel pore domain; CTD, C-terminal domain. Abbreviation of EMHG and VCEP criteria for variant classification: PMb, pathogenic moderate (PMb: Prevalence of the variant in an affected cohort is significantly increased ($P < 1 \times 10\text{-}7$) compared with the prevalence of a relevant low risk population); PPa, pathogenic supporting (Segregation with the IVCT phenotype in multiple affected (> 4) family members in a gene definitively known to cause the disease); PPb, pathogenic supporting (Computational evidence - conservation, evolutionary, impact of amino acid change - concordantly support a deleterious effect on the gene); PPc, pathogenic supporting (Association with a clinical reaction consistent with malignant hyperthermia under anesthesia and confirmed by a positive IVCT); BPa, benign supporting (Computational evidence - conservation, evolutionary, impact of amino acid change - concordantly suggest no impact on the gene or gene product); for a detailed description of VCEP criteria, see [6].

N.	Amino acid change	Nucleotide change	Exon	IVCT	REVEL score	PolyPhen-2 score	Grantham score	EMHG classification	VCEP classification	RyR1 domain	Allele Frequency	dbSNP
1	p.(Glu79Val)	c.236A>T	3	MHS	0.878	0.986	121	PPb (VUS)	PM1_moderate, PP3_moderate, Posterior Probability = 0.673 (VUS)	NTD-A	2.4e-7	-
2	p.(His460Gln)	c.1380C>G	13	MHS	0.624	1	24	PPc (VUS)	PM1_moderate, PS4_supporting Posterior probability = 0.501 (VUS)	N-Sol	4.00e-6	rs750304434
3	p.(Arg533Gly)	c.1597C>G	15	MHS	0.895	1	125	PMb, PPb (VUS)	PM1_moderate, PP3_moderate, Posterior probability 0.673 = (VUS)	N-Sol	not present	rs193922768
4	p.(Ile559Phe)	c.1675A>T	16	NT	0.909	1	21	PPb (VUS)	PP3_moderate Posterior probability = 0.323 (VUS)	N-Sol	not present	-
5	p.(His581Arg)	c.1742A>G	16	NT	0.908	1	29	PPb (VUS)	PP3_moderate Posterior probability = 0.323 (VUS)	N-Sol	not present	-
6	p.(Gln1279Lys)	c.3835C>A	28	MHS	0.72	0.996	53	PPc (VUS)	PS4_supporting Posterior probability = 0.189 (VUS)	SPRY3	7.00e-7	rs1249689187
7	p.(Arg2118Pro)	c.6353G>C	39	MHS/MHN in combination with p.(His2441Asp)	0.915	0.995	103	PPb, PPc (VUS)	PM1_moderate, PP3_ moderate, PS4_supporting, BS2_Moderate Posterior Probability = 0.502 (VUS)	J-Sol	2.00e-5	rs201649680
8	p.(Val2275Leu)	c.6823G>C	42	MHS	0.877	0.999	32	PMb, PPb (VUS)	PM1_moderate, PP3_moderate Posterior probability 0.673(VUS)	B-Sol	not present	-
9	p.(Asp2393Ala)	c.7178A>C	44	MHS	0.772	0.147	126	PMb, PPc (VUS)	PM1_moderate, PS_4 supporting Posterior probability = 0.501 (VUS)	B-Sol	6.2e-7	rs376251146
10	p.(His2441Asp)	c.7321C>G	45	MHS/MHN in combination with p.(Arg2118Pro)	0.752	0.981	81	PPb, PPc (VUS)	PM1_moderate, PS4_supporting, BS2_moderate Posterior Probability = 0.189 (VUS)	B-Sol	1.195e-5	rs142422765
11	p.(Asp2730Asn)	c.8188G>A	51	MHS	0.663	0.598	23	PMb, PPa (VUS)	(VUS)	B-Sol	not present	-
12	p.(Glu2835Asp)	c.8505A>T	54	NT	0.5	0.765	45	(VUS)	BP4_supporting Posterior probability = 0.089 (Likely benign)	B-Sol	3.11e-5	rs144777676
13	p.(Asp3102Gly)	c.9305A>G	63	MHS in combination with p.(Glu1175Lys and p.(Asp4505His)	0.92	0.952	94	PPb (VUS)	PP3_moderate Posterior probability = 0.323 (VUS)	B-Sol	2.4e-7	-
14	p.(Asp3242Asn)	c.9724G>A	66	NT	0.352	0.989	23	(VUS)	BP4_supporting Posterior probability = 0.089 (Likely benign)	B-Sol	8.04e-6	rs1231911930
15	p.(Thr3513Ala)	c.10537A>G	71	MHS in combination with p.(Thr2206Met)	0.383	0.001	58	BPa (VUS)	BP4_supporting Posterior probability = 0.089 (Likely benign)	B-Sol	not present	-
16	p.(Leu4018Pro)	c.12053T>C	88	MHS	0.72	1	98	PPc (VUS)	PS4_moderate Posterior probability = 0.323 (VUS)	C-Sol	not present	-
17	p.(Arg4201Gly)	c.12601C>G	90	MHS in combination with p.(Glu2764Lys)	0.61	0.995	125	PPb (VUS)	(VUS)	TaF	not present	-
18	p.(Ala4248Gly)	c.12743C>G	91	MHS	0.488	0.337	60	PMb, PPc (VUS)	PS4_supporting Posterior probability = 0.189 (VUS)	TaF	6.4e-7	-
19	p.(Asp4939Tyr)	c.14815G>T	103	NT	0.899	1	160	PPb (VUS)	PM1_supporting, PP3_supporting Posterior probability 0.329 (VUS)	Pore	not present	-

Table 2

Clinical and histological features of individuals carrying novel *RYR1* variants. The table lists novel variants identified either in single probands or in family members, diagnosed through IVCT combined with genetic analysis or by genetic analysis alone. Single probands are shown in white cells, while family members are grouped within shaded brown cells. Abbreviations: M, male; F, female; Not reported, history of general anesthesia not available; No general anesthesia, the individual had never undergone general anesthesia at the time of referral; CPK, creatine phosphate kinase; DPNH, nicotinamide adenine dinucleotide diaphorase.

Patient #	Family #	Gender	History of general anesthesia	Trigger in IVCT	Clinical data	Histological data	Amino acid change
1		M	No general anesthesia	Halothane and caffeine	CPK at rest 1034 U/l	No alterations	p.(Glu79Val)
2		M	General anesthesia with suspected MH reaction	Halothane and caffeine	-	Internal nuclei (1.71 %); fiber hypotrophy; target-like fibers negative for DPNH staining; prevalence of type II fibers	p.(His460Gln)
3	1	M	No general anesthesia	Halothane and caffeine	Rare muscular cramps	Internal nuclei (2 %); prevalence of type II fibers; fibers negative for DPNH staining	p.(Arg533Gly)
4	1	F	General anesthesia with no adverse events	Halothane and caffeine	CPK at rest 596 U/l	No internal nuclei; prevalence of type II fibers; fibers negative for DPNH staining	p.(Arg533Gly)
5		M	Not reported	Not Tested	-	-	p.(Ile559Phe)
6		F	Not reported	Not tested	-	-	p.(His581Arg)
7		F	General anesthesia with suspected MH reaction: increase in CPK after dantrolene administration	Halothane	-	No alterations	p.(Gln1279Lys)
8	2	M	Not reported	MHN	-	Prevalence of type II fibers	p.(Arg2118Pro) p.(His2441Asp)
9	2	M	General anesthesia with suspected MH reaction: increase in body temperature and End-Tidal CO_2, acidosis, and tachycardia	Halothane and caffeine	-	Myopathic signs with mitochondrial alterations	p.(Arg2118Pro) p.(His2441Asp)
10	2	M	Not reported	Halothane	-	Prevalence of type II fibers	p.(Arg2118Pro) p.(His2441Asp)
11		M	Not reported	Halothane and caffeine	Increased CPK at rest	Fiber hypotrophy	p.(Arg2118Pro)
12	3	F	Not reported	Not tested	-	-	p.(Val2275Leu)
13	3	M	Not reported	Halothane	Myalgia	Core and minicore-like structures	p.(Val2275Leu)
14	3	M	Not reported	Halothane	-	Prevalence of type II fibers	p.(Val2275Leu)
15	3	M	Not reported	Halothane	-	Presence of some atrophic fibers	p.(Val2275Leu)
16	3	M	No general anesthesia	Halothane and caffeine	-	-	p.(Val2275Leu)
17	4	F	No general anesthesia	Halothane	Myalgia	Moth eaten fibers	p.(Asp2393Ala)
18	4	M	General anesthesia with suspected MH reaction: increase in body temperature after anesthesia	Halothane	Increased CPK at rest	Prevalence of type II fibers	p.(Asp2393Ala)
19	5	F	No general anesthesia	Halothane	-	Moth-eaten fibers	p.(Asp2730Asn)
20	5	M	Not reported	Halothane	Myalgia	Fiber hypotrophy; prevalence of type II fibers	p.(Asp2730Asn)
21	5	M	Not reported	Halothane and caffeine	-	Minicore-like structure	p.(Asp2730Asn)
22	5	M	Not reported	Halothane	-	Minicore-like structure	p.(Asp2730Asn)
23	5	F	Not reported	Halothane and caffeine	-	Normal	p.(Asp2730Asn)
24		M	Not reported	Not tested	-	-	p.(Glu2835Asp)
25		M	Not reported	Halothane and caffeine	Increased CPK increased at rest	Ragged fibers	p.(Asp3102Gly) p.(Glu1175Lys) p.(Asp4505His
26		F	Not reported	Not tested	-	-	p.(Asp3242Asn)
27		M	Not reported	Halothane and caffeine	Increased CPK and rhabdomyolysis after exercise	Cores and minicore-like structure; internal nuclei	p.(Thr3513Ala) p.Thr2206Met
28		M	General anesthesia with suspected MH reaction: End-Tidal CO_2 41 mmHg, body temperature 39°C	Halothane and caffeine	-	Non-specific alterations	p.(Leu4018Pro)
29		M	Not reported	Not tested	-	-	p.(Arg4201Gly)
30		M	Not reported	Halothane e caffeine	Increased CPK at rest	Non-specific alterations	p.(Arg4201Gly) p.(Glu2764Lys)
31	6	M	General anesthesia with no adverse events	Caffeine	CPK at rest 300 U/l	No alterations	p.(Ala4248Gly)
32	6	M	General anesthesia with suspected MH reaction: acidosis, hypertension and increase in body temperature	Halothane	-	No alterations	p.(Ala4248Gly)
33	6	M	General anesthesia with no adverse events	Halothane	Muscle cramps at rest: CPK at rest 107 U/l	Internal nuclei (2 %); fiber hypotrophy; fibers with contractures	p.(Ala4248Gly)
34	6	M	General anesthesia with no adverse events	Halothane	Muscle cramps at rest; CPK at rest 250 U/l	Internal nuclei (1.8 %); prevalence of type II fibers	p.(Ala4248Gly)
35	6	F	Not reported	Not tested	-	-	p.(Ala4248Gly)

(*continued on next page*)

Table 2 (*continued*)

Patient #	Family #	Gender	History of general anesthesia	Trigger in IVCT	Clinical data	Histological data	Amino acid change
36	7	F	Not reported	Not tested	-	-	p.(Asp4939Tyr)
37	7	M	Not reported	Not tested	-	-	p.(Asp4939Tyr)

individual. He reported an increase in CPK levels at rest (up to 1024 U/l), while histological analysis revealed no muscle alteration. A similar variant, c.235G>A, changing Glu79 into Lys, was previously reported as probably damaging [38]. In silico analysis showed that the Glu79 residue is conserved among species and, according to REVEL and Polyphen-2 scores it can be classified as likely pathogenic.

The c.1380C>G variant in exon 13, resulting in the substitution of an His into Gln at residue 460, p.(His460Gln), was identified in a patient who tested positive in the IVCT and reported a previous unspecified adverse event during anesthesia. This individual did not report history of increased CPK levels. Histological analysis revealed the presence of hypotrophic fibers, target-like fibers negative for DPNH staining and prevalence of type II fibers.

A novel variant, c.3835C>A, (p.(Gln1279Lys)) was identified in exon 28 in an individual who tested positive to halothane but not to caffeine at the IVCT. She reported a MH reaction following general anesthesia with increase in CPK levels after dantrolene administration. Muscle biopsies revealed no alteration at the histological level.

Variant c.9305A>G in exon 63 results in the change of the highly conserved residue Asp3102 into a Gly, p.(Asp3102Gly). This variant was present in association with two known variants, c.3523G>A, p.(Glu1175Lys) and c.13513G>C, p.(Asp4505His) [genotype c.9305A>G; 3523G>A; 13513G>C] in one individual positive at the IVCT. He reported an increase in CPK levels at rest and the presence of ragged fibers at the histological level. The contribution of the three variants to the MHS phenotype has yet to be defined. The Asp3102Gly variant and p.(Glu1175Lys) variant can be classified as VUS according to the EMHG/VCEP score matrices, while p.(Asp4505His) is considered benign.

A variant in exon 71, c.10537A>G, resulting in the substitution of a Thr into an Ala at residue 3513, p.(Thr3513Ala) was identified in one MHS individual, who also carries the causative mutation p.(Thr2206Met). He reported an increase in CPK levels and rhabdomyolysis after exercise. Histological analysis of muscle biopsy revealed the presence of core-like structure and some internal nuclei, that can be ascribed to the p.(Thr2206Met), while the p.(Thr3513Ala) is considered likely benign according to the VCEP score matrix and VUS according to the EMHG criteria,

A variant in exon 88, c.12053T>C, resulting in the substitution of a Leu into a Pro at residue 4018, p.(Leu4018Pro) was identified in one MHS individual. He reported an MH reaction with End-Tidal CO_2 up to 41 mmHg and increase in body temperature up to 39°C. Muscle biopsy revealed no specific alteration at the histological analysis.

Variant c.12601C>G in exon 91, resulting in the substitution of an Arg into Gly at residue 4201, p.(Arg4201Gly) was identified in two individuals, of whom only one performed the IVCT and tested positive. This individual also carries variant c.8290G>A corresponding to p.(Glu2764Lys). The c.12601C>G variant is not present in population databases, where one additional variant in the same amino acid residue, the p.(Arg4201Cys) classified as VUS is reported. According to Polyphen2, this variant is considered as pathogenic, while it scores below the REVEL range to be considered as supporting pathogenic and is considered as VUS by the EMHG/VCEP pathogenicity classification scoring matrix.

3.3.1.3. Genetic analysis of individuals who did not underwent IVCT. 5 novel variants were identified in individuals who did not perform the IVCT.

The first variant, c.1675A>T, in exons 16, results in substitution of an Ile into Phe at residue 559, p.(Ile559Phe), while the second variant, c.1742A>G, also in in exons 16, results in the substitution of a His into Arg at residue 581, p.(His581Arg). Both variants are not present in population databases.

One variant, c.8505A>T was identified in exon 54, resulting in substitution of a Glu into Asp at residue 2835 (p.Glu2835Asp) his variant has an allele frequency of 3.11e-5 and is considered as VUS according to the EMHG criteria and likely benign by the VCEP score matrix.

One variant, c.9724G>A was identified in exon 66, resulting in substitution of an Asp into Asn at residue 3242 (p.Asp3242Asn). This variant is considered as VUS by the EMHG and likely benign according to the VCEP score matrix.

One variant, c.14815G>T was identified in exon 103, resulting in substitution of highly conserved Asp into Tyr at residue 4939, p.(Asp4939Tyr). This variant was identified in two members of a family.

3.3.1.4. Novel CACNA1S variants in MHS individuals. Analysis of the *CACNA1S* gene identified two novel variants. The first, c.3857T>C, reported as rs368079312 and resulting in the substitution of a Met into Thr at residue 1286, p.(Met1286Thr), was identified in a MHS individual. This variant is classified as likely pathogenic according to the EMHG/ACMG/AMP scoring matrix, with a Polyphen score of 1.000 and a frequency 9e-06 according to GnomAD.

The second, c.3026C>T, rs200224590, resulting in the substitution of a Thr into Met at residue 1009, p.(Thr1009Met), was identified in a MHS patient, who resulted positive only to caffeine, but not to halothane. This variant has a frequency of 1.39e-04, according to GnomAD and is classified as VUS according to the EMHG/pathogenicity classification matrix.

3.4. Localization of the novel RYR1 variants on the 3D channel structure

Superimposing pathogenic *RYR1* variants onto the channel's 3D structure has shown that amino acid substitutions are mostly present at critical regions that can induce alterations ranging from inter- and intra-domain interactions to changes in domain folding [30,39–43]. We therefore found of interest to localize the novel *RYR1* causative variants on the 3D channel structure aiming to verify whether their localization matched the region proposed to affect RYR1 channel functioning (Fig. 3, Fig. S2 and Table S3).

Of the 19 novel pathogenic variants reported in this manuscript, 6 variants are localized in the N-Terminal Domain A (NTD-A), N-terminal Solenoid (N-Sol) and SP1a/ryanodine receptor domain 3 (SPRY3) domains. The p.(Glu79Val) variant, in the NTD-A domain, might potentially impact on domain-domain interactions with the Central-Solenoid (C-Sol) domain (Fig. S3A), while the p.(His460Gln) variant in the N-Sol domain may alter inter-domain interaction with the C-sol (Fig. S3B). In contrast, the three variants p.(Arg533Gly), p.(Ile559Phe), and p.(His581Arg), all located in the N-Sol domain, may potentially disrupt intra-domain interactions (Fig. S3C-E). Finally, the p.(Gln1279Lys) variant, localized in the SPRY3 domain is predicted to affect interaction with the Bridging Solenoid (B-Sol)(Fig. S3F). In addition, the observation that the Gln1279 amino acid residue is located close to a region of divergence between RyR1 and RyR2 (Divergent Region 2 - DR2) may further support a role for this residue in regulation RyR1 activity [44,45].

B-Sol, C-Sol and Junctional Solenoid (J-Sol) domains form most of the cytoplasmic region of RYR1. In our cohort of patients, we identified a total of 10 novel *RYR1* variants, namely 1 in the J-Sol, 8 in the B-Sol, and

1 in the C-Sol domain. The p.(Arg2118Pro) variant identified in the J-Sol may potentially abolish interaction with the C-Sol domain and destabilize the helix where the Arg2118 is contained (Fig. S3G), while the p.(His2441Asp) variant, which was found in association with the p.(Arg2118Pro) variant, is located in a solvent-exposed area of the B-Sol domain (Fig. S3J). Among other variants present in the B-Sol, the p.(Val2275Leu) is part of a hydrophobic core and substitution with a Leu may affect the packing of this domain (Fig. S3H), while the p.(Asp2730Asn) is contained within a flexible linker that links the B-Sol to the Repeat34 domain (Fig. S3K). Finally, the p.(Asp3102Gly) is part of an alpha helix within the B-sol and mutation to Gly might break this helix, perturbing the folding and stability of the B-sol domain (Fig. S3L).

The p.(Leu4018Pro) variant is the only one present in the C-Sol domain. Mutation of Leu to Pro would affect the packing and may also break the alpha helix that Leu4019 is part of, thus destabilizing the folding of the C-Sol domain (Fig. S3M and S3O).

In the most C-terminal region of RyR1, three variants were identified: p.(Arg4201Gly) and p.(Ala4248Gly) are present in the Thumb and Forefinger domain (TaF) domain and p.(Asp4939Tyr) in the pore region (Fig. S3N and Fig. S3P). Although Arg4201 does not directly interact with the C-Sol, mutation to Gly likely destabilizes the alpha helix it is part of and likely affects the interactions with the C-terminal domain of RyR1. Asp4938 is part of the pore-lining S6 helix and makes salt bridge interactions with the S6 helix of a neighboring subunit. Mutation to Tyr would introduce substantial steric hindrance that affects the conformation of the pore and possibly the permeation of Ca^{2+} ions.

4. Discussion

While the IVCT remains the gold standard for MHS diagnosis in individuals who do not carry a validated pathogenic variant, during the last years, molecular genetic techniques based on NGS technologies have greatly improved the contribution of genetic analysis to MHS diagnosis, representing a valid and less invasive alternative diagnostic strategy. However, the potential of genetic diagnosis for MHS is still limited by the presence of many *RYR1* variants that lack diagnostic significance. Indeed, only a minority of these variants are currently classified as pathogenic or likely pathogenic according to EMHG and VCEP criteria [6,7,46].

Here, we report data from a 20-year analysis of a patient cohort tested at the Azienda Ospedaliera Universitaria Senese, which led to the identification of 19 novel *RYR1* variants. All cases carrying these variants were carefully evaluated according to EMHG and VCEP criteria, resulting in their classification as VUS, as they did not fully meet the requirements to be considered at least likely pathogenic for genetic diagnosis.

In the genetic screening conducted on individuals referred to our center for a MHS diagnosis, a total of 100 *RYR1* variants were identified. Seventy-five of these variants were found in individuals who had undergone an IVCT, while the remaining 25 were identified in patients referred to our center without prior IVCT testing.

More than 60 % of the referred individuals (824/1311) reported a family history of MHS. Among them, 293 underwent IVCT, with 160 testing positive. Genetic analysis of IVCT-positive individuals identified a pathogenic or likely pathogenic variant in over 60 % of them, a proportion consistent with literature reports indicating that 50–70 % of MHS individuals carry pathogenic variants [10,47]. This further supports the consensus that, in the context of familial MHS, genetic testing can be considered as a valuable and reliable tool that can significantly reduce the need for IVCT. In contrast, among individuals referred on the basis of elevated CPK levels (93 individuals), only 23 % received an MHS diagnosis by IVCT, and 35 % of them were found to carry a pathogenic *RYR1* variant, confirming that hyperCKemia is not a specific predictor of MHS. Finally, only one-third of individuals referred to our center for a suspected MHS reaction during anesthesia tested positive at the IVCT (11/36), indicating that clinical recognition of MHS signs still needs to be improved.

Among the 100 variants identified in *RYR1*, 34 can be classified as pathogenic or likely pathogenic according to the analysis reported by Johnston et al., 2022 [7]. Of these, 30 variants are included in the list of the EMHG diagnostic variants, based on both genetic and functional characterization. Among those variants considered pathogenic or likely pathogenic according to VCEP criteria, but not included in the EMHG list, three [p.(Glu1175Lys), p.(Gly2375Arg) and p.(Val2627Met)] were identified in individuals positive to IVCT, further supporting their potential causative role in MHS.

In addition, EMHG and VCEP classifications are not fully aligned for the variant p.(Pro4973Leu) that is included in the EMHG list of causative variants but is considered a VUS according to VCEP [7].

Another variant, the c.14051T>C, p.(Phe4684Ser), was previously identified in individuals with MHS [23,48,49]. Despite a high PolyPhen-2 score of 0.998, it is classified as VUS by VCEP and it is not included in the EMHG list, likely due to lack of functional data. We identified this variant in a family in which 7 out of 8 IVCT-positive members carried the variant and one proband experienced a suspected MH event. It is reasonable to consider the IVCT-positive individual who lacks the variant as a potential false positive.

Initial identification of disease-causing *RYR1* mutations revealed that most mutations were mainly clustered in three distinct “hot spots” [the N-terminal (MH1), central (MH2), and C-terminal (MH3) regions] suggesting that these areas may contain key regulatory domains essential for channel function [8,30,41,50,51]. With time, several variants have been identified also outside these hot spots. Indeed, current knowledge based on the available cryo-EM reconstruction of RYR1 channels has revealed that each RYR1 protomer contains several structural domains along the entire lengths of the protein that help in assembling the functional tetrameric channel [40,41,43,44]. Studies comparing channel structures in open and closed states, have shown that the functional transition between closed and open conformations results from a continuum of structural changes involving interconnected domains, which ultimately regulate the probability of channel opening. With respect to the three hot spot regions, the 19 novel variants reported in this study are distributed as follows, 5 in MH1, 4 in MH2 and 1 in MH3, while the remaining 9 are located outside these regions. Mapping of the novel variants onto the 3D structure revealed that most of them are predicted to affect either inter- or intra-domain interactions, or alter domain folding, supporting the outcomes of other predictive tools. Most of the novel variants were identified in the B-Sol domain of RYR1 (8 variants), that together with the J-Sol and C-Sol domains, where we identified 2 additional variants, form the largest part of the cytoplasmic shell of RYR1. These data are in line with literature data that report that 24 of 91 variants identified in the B-Sol domain can be classified as likely pathogenic [7,8,30,52].

The routine use of NGS technologies for genetic analysis has also led to the occasional identification of multiple variants within the same gene. Interestingly, although most of the individuals evaluated in this retrospective analysis carried a single variant in *RYR1*, we also identified two families and three unrelated probands harboring two or even three different variants.

Unfortunately, we could not establish whether the multiple variants were present in cis or in trans. In two cases, assessment of family history and literature data enabled us to infer a more significant role for one variant over the other. In one proband carrying both the p.(Thr3513Ala) and p.(Thr2206Met) variants, the causative role of the latter was confirmed [49,53–55], while p.(Thr3513Ala) is classified as VUS according to the EMHG/VCEP score matrix. On the other hand, predictions from REVEL and PolyPhen-2 suggest that this variant may be considered as likely benign, thus indicating that its role on the MHS phenotype may be minimal, if any.

In a second family, where two members resulted MHS at the IVCT, one member carried two variants p.(Glu2362Gly) and p.(Asp4505His), while the second one only carried the p.(Glu2362Gly), thus allowing us

to exclude the causative role of p.(Asp4505His). Indeed, it should be noted that although the p.(Asp4505His) variant is classified as benign by ClinGen, an increase in caffeine sensitivity in *in vitro* studies has been reported for this variant [16]. The p.(Asp4505His) variant was also identified in one MHS individual in combination with two other variants, p.(Asp3102Gly) and p.(Glu1175Lys). In this case, we could not exclude the role of either one of the two other variants. According to 3D mapping, they are both predicted to destabilize inter-domain interactions, folding and stability of the B-Sol domain. In addition, p.(Glu1175Lys) has been previously reported in patients with congenital myopathy [56,57]; however, since in these patients, p.(Glu1175Lys) variant was identified in combination with other *RYR1* variants, its contribution to MHS remains to be established. The contribution of p.(Asp3102Gly) alone is also to be evaluated since this variant is novel.

In a family with three MHS members, two variants, p.(Arg2118Pro) and p.(His2441Asp), were identified; one member experienced an MH crisis during general anesthesia. Notably, the p.(Arg2118Pro) variant alone was also detected in an unrelated individual diagnosed as MHS. A variant changing Arg2118 to Trp, p.(Arg2118Trp) was identified in combination with a second *RYR1* variant in patients with congenital myopathies with or without cores and minicores [52,58]. Data from 3D mapping predicts that mutation of Arg2118 may abolish intra-domain interactions, while the same analysis indicates that the impact of the second variant p.(His2441Asp) is expected to be minimal. This is consistent with the observation that the p.(Arg2118Pro) variant, when present alone was sufficient to elicit a positive response to IVCT. These findings may, therefore, support the notion that p.(Arg2118Pro) can potentially exert a stronger causative effect on the MHS phenotype than p.(His2441Asp).

Finally, the combined role of the two variants p.(Arg4201Gly) and p.(Glu2764Lys) also needs to be further evaluated, since the p.(Arg4201Gly) is novel and predicted to impact on intra-domains interactions, while p.(Glu2764Lys), although expected not to have a significant role on RYR1 structure, was previously identified in a patient with primary periodic paralysis [59] and in another MHS patient [23]. In addition, we identified an individual at our center carrying only the p.(Arg4201Gly) variant; however, this subject was not evaluated by IVCT.

The two novel variants in *CACNA1S*, p.(Thr2009Met) and p.(Met1286Thr) are located in the intramembrane S5-S6 loop forming the channel's selectivity filter, and within a pore-forming region and in helix S5 of repeat IV, respectively [60]. Although Thr2009 is highly conserved across species, in silico predictions yield conflicting classification: REVEL and PolyPhen classify this variant as moderately pathogenic and probably damaging, respectively, whereas AlphaMissense [61] suggests a likely benign interpretation. In contrast, p.(Met1286Thr) is consistently predicted by these programs as likely pathogenic by all tools assessed with high confident scores.

Interestingly, in 38 of the MHS individuals, no mutations were identified in *RYR1, CACNA1S, STAC3*, or in any of the 16 additional genes included in the NGS panel that encode proteins associated with excitation–contraction coupling, further supporting the current understanding that other genes may be associated with MH.

The data presented in this study indicate that the number of known *RYR1* and *CACNA1S* variants potentially associated with MHS is continuously increasing. Consequently, careful evaluation is required when classifying variants in the context of genetic diagnosis for MHS. The interpretation of *RYR1* variants remains particularly challenging due to the complexity of functional *in vitro* studies and the limited availability of detailed clinical information for some identified variants. Periodic re-evaluation of known variants, in light of newly reported functional or clinical evidence, represents an essential practice to improve and refine the molecular diagnosis of MHS. Indeed, following recent updates by the EMHG/VCEP regarding the classification of pathogenic and likely pathogenic variants, we re-examined the genetic findings of 20 individuals who had previously been reported to carry variants previously classified as VUS.

In conclusion, we report here available clinical and familial data for 19 novel *RYR1* and 2 *CACNA1S* variants currently classified as VUS. Data sharing between laboratories may help further refining the classification of these and other VUS, either by confirming their current status or by supporting their reclassification as benign/likely benign or likely pathogenic/pathogenic.

CRediT authorship contribution statement

Daniela Rossi: Writing – review & editing, Writing – original draft, Supervision, Formal analysis, Data curation. **Carlotta Pranzo:** Data curation. **Sara Roccabianca:** Data curation. **Lucia Galli:** Methodology, Formal analysis. **Alfredo Orrico:** Formal analysis, Data curation. **Giovanna Sorbello:** Methodology. **Vincenzo Tegazzin:** Methodology, Formal analysis. **Pasquale D'Onofrio:** Supervision. **Armando Fucci:** Methodology. **Salvatore Quarta:** Methodology. **Stefano Perni:** Supervision. **Egidio Maria Rubino:** Supervision. **Matteo Serano:** Supervision. **Gianna Berti:** Methodology. **Diego Lopergolo:** Supervision. **Alessandro Malandrini:** Supervision, Formal analysis. **Filip Van Petegem:** Methodology, Formal analysis. **Vincenzo Sorrentino:** Writing – review & editing, Supervision, Resources.

Declaration of competing interest

None

Acknowledgments

This research was funded by grants to V. Sorrentino from the Center for Gene Therapy and Drugs Based on RNA Technology, funded in the framework of the National Recovery and Resilience Plan (NRRP), M4C2 Inv, 1.4 CUP B63C22000610006 - Spoke 1", from the Tuscan Health Ecosystem, funded in the framework of the National Recovery and Resilience Plan (NRRP), Missione 4 Componente 2 Inv. 1.5 CUP B63C22000680007 - Spoke 7". Both grants are funded by the European Union-Next Generation EU program. Additional grants are from Association Française contre les Myopathies -AFM- (Grants 29433 to VS and 24835 to DR) and from Italian Ministry of University (PRIN) to DR.

Supplementary materials

Supplementary material associated with this article can be found, in the online version, at doi:10.1016/j.nmd.2025.106296.

References

[1] Larach MG, Localio AR, Allen GC, Denborough MA, Ellis FR, Gronert GA, et al. A Clinical Grading Scale to Predict Malignant Hyperthermia Susceptibility. Anesthesiology 1994;80:771–9. https://doi.org/10.1097/00000542-199404000-00008.

[2] Larach MG, Gronert GA, Allen GC, Brandom BW, Lehman EB. Clinical Presentation, Treatment, and Complications of Malignant Hyperthermia in North America from 1987 to 2006. Anesth Analg 2010;110:498–507. https://doi.org/10.1213/ANE.0b013e3181c6b9b2.

[3] Hopkins PM, Rüffert H, Snoeck MM, Girard T, Glahn KPE, Ellis FR, et al. European Malignant Hyperthermia Group guidelines for investigation of malignant hyperthermia susceptibility. Br J Anaesth 2015;115:531–9. https://doi.org/10.1093/bja/aev225.

[4] Hopkins PM, Girard T, Dalay S, Jenkins B, Thacker A, Patteril M, et al. Malignant hyperthermia 2020. Anaesthesia 2021;76:655–64. https://doi.org/10.1111/anae.15317.

[5] Ellinas H, Albrecht MA. Malignant Hyperthermia Update. Anesthesiol Clin 2020;38:165–81. https://doi.org/10.1016/j.anclin.2019.10.010.

[6] Johnston JJ, Dirksen RT, Girard T, Gonsalves SG, Hopkins PM, Riazi S, et al. Variant curation expert panel recommendations for RYR1 pathogenicity classifications in malignant hyperthermia susceptibility. Genet Med 2021;23:1288–95. https://doi.org/10.1038/s41436-021-01125-w.

[7] Johnston JJ, Dirksen RT, Girard T, Hopkins PM, Kraeva N, Ognoon M, et al. Updated variant curation expert panel criteria and pathogenicity classifications for 251 variants for *RYR1* -related malignant hyperthermia susceptibility. Hum Mol Genet 2022;31:4087–93. https://doi.org/10.1093/hmg/ddac145.

[8] Rossi D, Catallo MR, Pierantozzi E, Sorrentino V. Mutations in proteins involved in E-C coupling and SOCE and congenital myopathies. J Gen Physiol 2022;154. https://doi.org/10.1085/jgp.202213115.

[9] Hoppe K, Jurkat-Rott K, Kranepuhl S, Wearing S, Heiderich S, Merlak S, et al. Relevance of pathogenicity prediction tools in human RYR1 variants of unknown significance. Sci Rep 2021;11:3445. https://doi.org/10.1038/s41598-021-82024-7.

[10] Riazi S, Kraeva N, Hopkins PM. Malignant Hyperthermia in the Post-Genomics Era. Anesthesiology 2018;128:168–80. https://doi.org/10.1097/ALN.0000000000001878.

[11] Barone V, Mazzoli E, Kunic J, Rossi D, Tronnolone S, Sorrentino V. Yip1B isoform is localized at ER–Golgi intermediate and cis-Golgi compartments and is not required for maintenance of the Golgi structure in skeletal muscle. Histochem Cell Biol 2015;143:235–43. https://doi.org/10.1007/s00418-014-1277-z.

[12] O'Connor TN, van den Bersselaar LR, Chen YS, Nicolau S, Simon B, Huseth A, et al. RYR-1-Related Diseases International Research Workshop: From Mechanisms to Treatments Pittsburgh, PA, U.S.A., 21-22 July 2022. J Neuromuscul Dis 2023;10:135–54. https://doi.org/10.3233/JND-221609.

[13] Ibarra Moreno CA, Silva HCA, Voermans NC, Jungbluth H, van den Bersselaar LR, Rendu J, et al. Myopathic manifestations across the adult lifespan of patients with malignant hyperthermia susceptibility: a narrative review. Br J Anaesth 2024;133:759–67. https://doi.org/10.1016/j.bja.2024.05.046.

[14] Protasi F, Girolami B, Roccabianca S, Rossi D. Store-operated calcium entry: From physiology to tubular aggregate myopathy. Curr Opin Pharmacol 2023;68:102347. https://doi.org/10.1016/j.coph.2022.102347.

[15] Wappler F, Fiege M, Steinfath M, Agarwal K, Scholz J, Singh S, et al. Evidence for Susceptibility to Malignant Hyperthermia in Patients with Exercise-induced Rhabdomyolysis. Anesthesiology 2001;94:95–100. https://doi.org/10.1097/00000542-200101000-00019.

[16] Groom L, Muldoon SM, Tang ZZ, Brandom BW, Bayarsaikhan M, Bina S, et al. Identical de novo Mutation in the Type 1 Ryanodine Receptor Gene Associated with Fatal, Stress-induced Malignant Hyperthermia in Two Unrelated Families. Anesthesiology 2011;115:938–45. https://doi.org/10.1097/ALN.0b013e3182320068.

[17] Dlamini N, Voermans NC, Lillis S, Stewart K, Kamsteeg E-J, Drost G, et al. Mutations in RYR1 are a common cause of exertional myalgia and rhabdomyolysis. Neuromuscul Disord 2013;23:540–8. https://doi.org/10.1016/j.nmd.2013.03.008.

[18] Timmins MA, Rosenberg H, Larach MG, Sterling C, Kraeva N, Riazi S. Malignant Hyperthermia Testing in Probands without Adverse Anesthetic Reaction. Anesthesiology 2015;123:548–56. https://doi.org/10.1097/ALN.0000000000000732.

[19] Zvaritch E, Gillies R, Kraeva N, Richer M, Jungbluth H, Riazi S. Fatal awake malignant hyperthermia episodes in a family with malignant hyperthermia susceptibility: a case series. Canad J Anesthesia/J Canadien d'anesthésie 2019;66:540–5. https://doi.org/10.1007/s12630-019-01320-z.

[20] Gardner L, Miller DM, Daly C, Gupta PK, House C, Roiz de Sa D, et al. Investigating the genetic susceptibility to exertional heat illness. J Med Genet 2020;57:531–41. https://doi.org/10.1136/jmedgenet-2019-106461.

[21] Allen GC, Larach MG, Kunselman AR. The Sensitivity and Specificity of the Caffeine-Halothane Contracture Test. Anesthesiology 1998;88:579–88. https://doi.org/10.1097/00000542-199803000-00006.

[22] Rossi D, Gigli L, Gamberucci A, Bordoni R, Pietrelli A, Lorenzini S, et al. A novel homozygous mutation in the TRDN gene causes a severe form of pediatric malignant ventricular arrhythmia. Heart Rhythm 2020;17:296–304. https://doi.org/10.1016/j.hrthm.2019.08.018.

[23] Galli L, Orrico A, Lorenzini S, Censini S, Falciani M, Covacci A, et al. Frequency and localization of mutations in the 106 exons of theRYR1 gene in 50 individuals with malignant hyperthermia. Hum Mutat 2006;27. https://doi.org/10.1002/humu.9442. 830–830.

[24] Adzhubei IA, Schmidt S, Peshkin L, Ramensky VE, Gerasimova A, Bork P, et al. A method and server for predicting damaging missense mutations. Nat Methods 2010;7:248–9. https://doi.org/10.1038/nmeth0410-248.

[25] Ioannidis NM, Rothstein JH, Pejaver V, Middha S, McDonnell SK, Baheti S, et al. REVEL: An Ensemble Method for Predicting the Pathogenicity of Rare Missense Variants. The Am J Human Genet 2016;99:877–85. https://doi.org/10.1016/j.ajhg.2016.08.016.

[26] Richards S, Aziz N, Bale S, Bick D, Das S, Gastier-Foster J, et al. Standards and guidelines for the interpretation of sequence variants: a joint consensus recommendation of the American College of Medical Genetics and Genomics and the Association for Molecular Pathology. Genet Med 2015;17:405–24. https://doi.org/10.1038/gim.2015.30.

[27] Kopanos C, Tsiolkas V, Kouris A, Chapple CE, Albarca Aguilera M, Meyer R, et al. VarSome: the human genomic variant search engine. Bioinformatics 2019;35:1978–80. https://doi.org/10.1093/bioinformatics/bty897.

[28] Vattemi GNA, Rossi D, Galli L, Catallo MR, Pancheri E, Marchetto G, et al. Ryanodine receptor 1 (*RYR1*) mutations in two patients with tubular aggregate myopathy. Eur J Neurosci 2022;56:4214–23. https://doi.org/10.1111/ejn.15728.

[29] Melville Z, Kim K, Clarke OB, Marks AR. High-resolution structure of the membrane-embedded skeletal muscle ryanodine receptor. Structure 2022;30:172–80. https://doi.org/10.1016/j.str.2021.08.001. e3.

[30] Woll KA, Haji-Ghassemi O, Van Petegem F. Pathological conformations of disease mutant Ryanodine Receptors revealed by cryo-EM. Nat Commun 2021;12:807. https://doi.org/10.1038/s41467-021-21141-3.

[31] Lau K, Van Petegem F. Crystal structures of wild type and disease mutant forms of the ryanodine receptor SPRY2 domain. Nat Commun 2014;5:5397. https://doi.org/10.1038/ncomms6397.

[32] Kojima Y, Oku S, Takahashi K, Mukaida K. Susceptibility to Malignant Hyperthermia Manifested as Delayed Return of Increased Serum Creatine Kinase Activity and Episodic Rhabdomyolysis after Exercise. Anesthesiology 1997;87:1565–7. https://doi.org/10.1097/00000542-199712000-00035.

[33] Santos JM, Andrade PV, Galleni L, Vainzof M, Sobreira CFR, Schmidt B, et al. Idiopathic hyperCKemia and malignant hyperthermia susceptibility. Canad J Anesth/J Canadien d'anesthésie 2017;64:1202–10. https://doi.org/10.1007/s12630-017-0978-x.

[34] Weglinski MR, Wedel DJ, Engel AG. Malignant Hyperthermia Testing in Patients with Persistently Increased Serum Creatine Kinase Levels. Anesth Analg 1997;84:1038–41. https://doi.org/10.1097/00000539-199705000-00016.

[35] Ellis FR, Clarke IM, Modgill M, Currie S, Harriman DG. Evaluation of creatinine phosphokinase in screening patients for malignant hyperpyrexia. BMJ 1975;3:511–3. https://doi.org/10.1136/bmj.3.5982.511.

[36] Malandrini A, Orrico A, Gaudiano C, Gambelli S, Galli L, Berti G, et al. Muscle Biopsy and In Vitro Contracture Test in Subjects with Idiopathic HyperCKemia. Anesthesiology 2008;109:625–8. https://doi.org/10.1097/ALN.0b013e3181862a0d.

[37] Knuiman GJ, Küsters B, Eshuis L, Snoeck M, Lammens M, Heytens L, et al. The histopathological spectrum of malignant hyperthermia and rhabdomyolysis due to RYR1 mutations. J Neurol 2019;266:876–87. https://doi.org/10.1007/s00415-019-09209-z.

[38] Coburger J, Kapapa T, Wirtz CR, Jurkat-Rott K, Klingler W. High prevalence of rare ryanodine receptor type 1 variants in patients suffering from aneurysmatic subarachnoid hemorrhage: A pilot study. J Clin Neurosci 2017;45:209–13. https://doi.org/10.1016/j.jocn.2017.06.029.

[39] Zalk R, Clarke OB, des Georges A, Grassucci RA, Reiken S, Mancia F, et al. Structure of a mammalian ryanodine receptor. Nature 2015;517:44–9. https://doi.org/10.1038/nature13950.

[40] des Georges A, Clarke OB, Zalk R, Yuan Q, Condon KJ, Grassucci RA, et al. Structural Basis for Gating and Activation of RyR1. Cell 2016;167:145–57. https://doi.org/10.1016/j.cell.2016.08.075. e17.

[41] Ma R, Haji-Ghassemi O, Ma D, Jiang H, Lin L, Yao L, et al. Structural basis for diamide modulation of ryanodine receptor. Nat Chem Biol 2020;16:1246–54. https://doi.org/10.1038/s41589-020-0627-5.

[42] Ponting C. SPRY domains in ryanodine receptors (Ca2+-release channels). Trends Biochem Sci 1997;22:193–4. https://doi.org/10.1016/S0968-0004(97)01049-9.

[43] Woll KA, Van Petegem F. Calcium-release channels: structure and function of IP 3 receptors and ryanodine receptors. Physiol Rev 2022;102:209–68. https://doi.org/10.1152/physrev.00033.2020.

[44] Samsó M. A guide to the 3D structure of the ryanodine receptor type 1 by cryoEM. Protein Sci 2017;26:52–68. https://doi.org/10.1002/pro.3052.

[45] Sorrentino V, Volpe P. Ryanodine receptors: how many, where and why? Trends Pharmacol Sci 1993;14:98–103. https://doi.org/10.1016/0165-6147(93)90072-r.

[46] Gonsalves SG, Ng D, Johnston JJ, Teer JK, Stenson PD, Cooper DN, et al. Using exome data to identify malignant hyperthermia susceptibility mutations. Anesthesiology 2013;119:1043–53. https://doi.org/10.1097/ALN.0b013e3182a8a8e7.

[47] Miller DM, Daly C, Aboelsaod EM, Gardner L, Hobson SJ, Riasat K, et al. Genetic epidemiology of malignant hyperthermia in the UK. Br J Anaesth 2018;121:944–52. https://doi.org/10.1016/j.bja.2018.06.028.

[48] MacLennan DH, Zvaritch E. Mechanistic models for muscle diseases and disorders originating in the sarcoplasmic reticulum. Biochim Biophys Acta (BBA) - Mol Cell Res 2011;1813:948–64. https://doi.org/10.1016/j.bbamcr.2010.11.009.

[49] Monnier N, Kozak-Ribbens G, Krivosic-Horber R, Nivoche Y, Qi D, Kraev N, et al. Correlations between genotype and pharmacological, histological, functional, and clinical phenotypes in malignant hyperthermia susceptibility. Hum Mutat 2005;26:413–25. https://doi.org/10.1002/humu.20231.

[50] Iyer KA, Hu Y, Klose T, Murayama T, Samsó M. Molecular mechanism of the severe MH/CCD mutation Y522S in skeletal ryanodine receptor (RyR1) by cryo-EM. Proc Natl Acad Sci 2022;119. https://doi.org/10.1073/pnas.2122140119.

[51] Rossi D, Sorrentino V. Molecular genetics of ryanodine receptors Ca2+-release channels. Cell Calcium 2002;32:307–19. https://doi.org/10.1016/S0143416002001987.

[52] Fusto A, Cassandrini D, Fiorillo C, Codemo V, Astrea G, D'Amico A, et al. Expanding the clinical-pathological and genetic spectrum of RYR1-related congenital myopathies with cores and minicores: an Italian population study. Acta Neuropathol Commun 2022;10:54. https://doi.org/10.1186/s40478-022-01357-0.

[53] Klingler W, Heiderich S, Girard T, Gravino E, Heffron JJ, Johannsen S, et al. Functional and genetic characterization of clinical malignant hyperthermia crises: a multi-centre study. Orphanet J Rare Dis 2014;9:8. https://doi.org/10.1186/1750-1172-9-8.

[54] Treves S, Anderson AA, Ducreux S, Divet A, Bleunven C, Grasso C, et al. Ryanodine receptor 1 mutations, dysregulation of calcium homeostasis and neuromuscular disorders. Neuromuscul Disord 2005;15:577–87. https://doi.org/10.1016/j.nmd.2005.06.008.

[55] Wehner M, Rueffert H, Koenig F, Neuhaus J, Olthoff D. Increased sensitivity to 4-chloro-m-cresol and caffeine in primary myotubes from malignant hyperthermia susceptible individuals carrying the ryanodine receptor 1 Thr2206Met (C6617T) mutation. Clin Genet 2002;62:135–46. https://doi.org/10.1034/j.1399-0004.2002.620206.x.

[56] de Feraudy Y, Vandroux M, Romero NB, Schneider R, Saker S, Boland A, et al. Exome sequencing in undiagnosed congenital myopathy reveals new genes and refines genes–phenotypes correlations. Genome Med 2024;16:87. https://doi.org/10.1186/s13073-024-01353-0.

[57] Abath Neto O, Moreno C de AM, Malfatti E, Donkervoort S, Böhm J, Guimarães JB, et al. Common and variable clinical, histological, and imaging findings of recessive RYR1-related centronuclear myopathy patients. Neuromuscul Disord 2017;27:975–85. https://doi.org/10.1016/j.nmd.2017.05.016.

[58] Fattori F, Maggi L, Bruno C, Cassandrini D, Codemo V, Catteruccia M, et al. Centronuclear myopathies: genotype–phenotype correlation and frequency of defined genetic forms in an Italian cohort. J Neurol 2015;262:1728–40. https://doi.org/10.1007/s00415-015-7757-9.

[59] Luo S, Xu M, Sun J, Qiao K, Song J, Cai S, et al. Identification of gene mutations in patients with primary periodic paralysis using targeted next-generation sequencing. BMC Neurol 2019;19:92. https://doi.org/10.1186/s12883-019-1322-6.

[60] Flucher BE. Skeletal muscle CaV1.1 channelopathies. Pflugers Arch 2020;472:739–54. https://doi.org/10.1007/s00424-020-02368-3.

[61] Jumper J, Evans R, Pritzel A, Green T, Figurnov M, Ronneberger O, et al. Highly accurate protein structure prediction with AlphaFold. Nature 2021;596:583–9. https://doi.org/10.1038/s41586-021-03819-2.